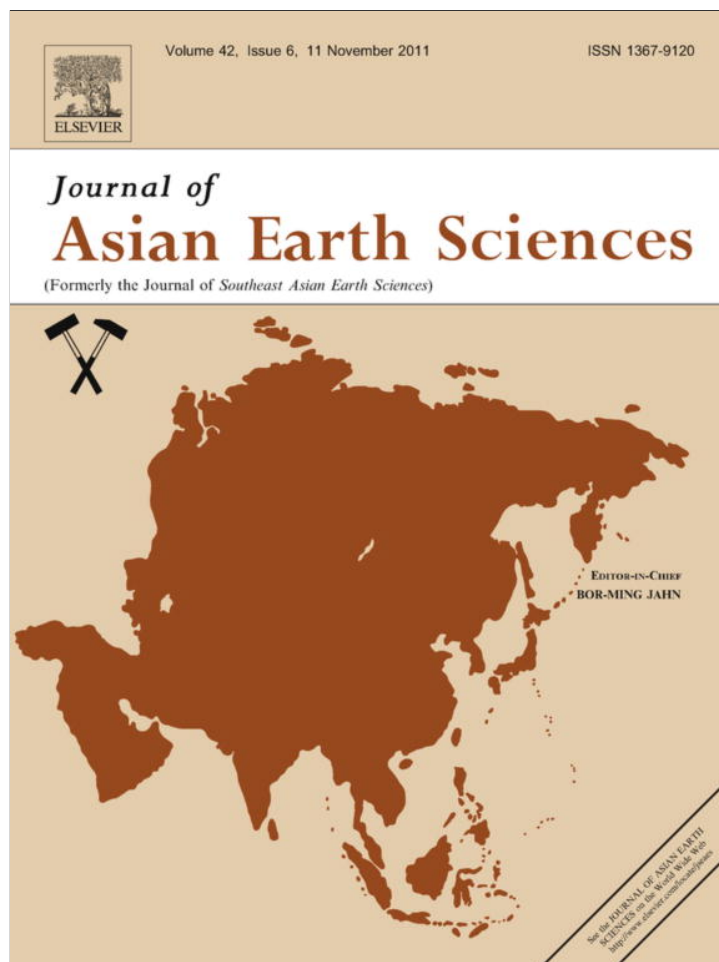


Provided for non-commercial research and education use.  
Not for reproduction, distribution or commercial use.



This article appeared in a journal published by Elsevier. The attached copy is furnished to the author for internal non-commercial research and education use, including for instruction at the authors institution and sharing with colleagues.

Other uses, including reproduction and distribution, or selling or licensing copies, or posting to personal, institutional or third party websites are prohibited.

In most cases authors are permitted to post their version of the article (e.g. in Word or Tex form) to their personal website or institutional repository. Authors requiring further information regarding Elsevier's archiving and manuscript policies are encouraged to visit:

<http://www.elsevier.com/copyright>



Contents lists available at SciVerse ScienceDirect

## Journal of Asian Earth Sciences

journal homepage: [www.elsevier.com/locate/jseas](http://www.elsevier.com/locate/jseas)

## $^{57}\text{Fe}$ Mössbauer spectroscopic analysis of deep-sea pelagic chert: Effect of secondary alteration with respect to paleo-redox evaluation

Tomohiko Sato<sup>a,\*</sup>, Yukio Isozaki<sup>a</sup>, Katsumi Shozugawa<sup>b</sup>, Motoyuki Matsuo<sup>b</sup><sup>a</sup> Department of Earth Science and Astronomy, Graduate School of Arts and Sciences, The University of Tokyo, 3-8-1 Komaba, Meguro, Tokyo, Japan<sup>b</sup> Department of Chemistry, Graduate School of Arts and Sciences, The University of Tokyo, 3-8-1 Komaba, Meguro, Tokyo, Japan

## ARTICLE INFO

## Article history:

Received 6 May 2011

Received in revised form 27 July 2011

Accepted 8 August 2011

Available online 16 August 2011

## Keywords:

Deep-sea chert

Redox

Iron

Alteration

Mössbauer spectroscopy

Triassic

## ABSTRACT

Chemical states of iron in the pre-Jurassic pelagic deep-sea cherts are used as one of redox indicators of lost deep-oceans, e.g. the Permian–Triassic boundary case. Primarily red hematite-bearing cherts were often altered secondarily into greenish gray cherts. We examined the pattern of secondary change in chemical state of iron, associated with color change, in the Middle Triassic chert beds at Hisuikyo in central Japan by  $^{57}\text{Fe}$  Mössbauer spectroscopy. Three sets of chert bed with the lateral color change from red to greenish gray were analyzed. The analyses confirmed that the red cherts contain hematite, paramagnetic  $\text{Fe}^{3+}$ , and paramagnetic  $\text{Fe}^{2+}$ , whereas the greenish gray cherts contain paramagnetic  $\text{Fe}^{3+}$  and paramagnetic  $\text{Fe}^{2+}$  without hematite. The greenish gray parts contain larger amounts of paramagnetic  $\text{Fe}^{2+}$  component of amorphous siderite-like mineral, in contrast to the red parts have lesser amounts. These results confirmed that the primary hematite has changed into paramagnetic  $\text{Fe}^{2+}$ -bearing minerals, in accordance with the color change, by the secondary alteration. Further comparison with the pyrite-bearing primary black to dark-gray cherts was discussed with respect to the evaluation for primary redox change in the past oceans.

© 2011 Elsevier Ltd. All rights reserved.

## 1. Introduction

In monitoring paleo-oceanic environments with respect to the evolution of life, changes in sea-water redox in the past ocean has drawn special attention for years (e.g., Anbar and Knoll, 2002; Holland, 2006; Shields and Och, 2011). Direct geological information for the Precambrian to Paleozoic deep oceans has not been easily checked, however, simply because all deep-sea floors prior to the Early Jurassic were completely lost by oceanic subduction. Deep-sea pelagic cherts contained in on-land exposed accretionary complexes (Matsuda and Isozaki, 1991), although minor in amount, can solve this deadlock by provide extremely rare records of ancient deep-sea floors, in particular, of the pre-Jurassic age, as first pointed out for the Permian–Triassic (P–T) boundary study in Japan (e.g. Isozaki, 1994, 1997a).

Bedded chert in accretionary complex is composed mostly of fine-grained quartz (usually over 90 wt.% up to 95 wt.% of  $\text{SiO}_2$  in bulk chemistry). In other words, chert is a mineralogically simple sedimentary rock, of which major chemical composition unlikely reflects sensitive redox changes. In contrast, some accessory iron-bearing minerals in bedded chert can be used as a redox indicator for ancient deep oceans, as preliminarily performed by Nakao and

Isozaki (1994), Kubo et al. (1996), and Matsuo et al. (2003). These works demonstrated that red cherts with hematite were primarily deposited under oxidizing conditions, whereas pyrite-bearing black to dark-gray cherts under reducing conditions. As most of the unmetamorphosed/unaltered Late Paleozoic and Mesozoic bedded cherts in on-land exposed accretionary complexes are red in color, oxidizing conditions likely persisted in deep-ocean throughout the Late Paleozoic to Mesozoic, except for some unique intervals of reducing conditions, such as the P–T Superanoxic period (e.g. Isozaki, 1994, 1997a) and the Toarcian (Early Jurassic) oceanic anoxic event (e.g. Hori, 1993). These results were partly confirmed by analyses of sulfur isotope ratio and of rare earth element (REE) abundance pattern (e.g., Kajiwarra et al., 1994; Ishiga et al., 1996; Kato et al., 2002; Kakuwa, 2008; Algeo et al., 2011).

In evaluating proper paleo-redox from ancient deep-sea cherts, however, secondary alteration of chert and its effect in iron-bearing minerals remain as an issue to be checked. We often observe some examples of lateral color changes from red into greenish gray within a single bed in the chert outcrops, which apparently demonstrate the consequence of secondary alteration after deposition. Detailed field observations confirmed that the change is always from red to greenish gray, but never *vice versa*. Post-lithification diagenesis with water infiltration (e.g. Thurston, 1972; Umeda, 1999) is a possible explanation for this color change, nonetheless, analyses of quantitative chemistry and mineralogy have not yet

\* Corresponding author. Tel.: +81 3 5454 6365; fax: +81 3 5465 8244.

E-mail address: [tomohiko@ea.c.u-tokyo.ac.jp](mailto:tomohiko@ea.c.u-tokyo.ac.jp) (T. Sato).

been performed to confirm this alleged secondary alteration processes and results.

The mineralogical characterization of non-red colored cherts is particularly significant in assessing paleo-redox because typical

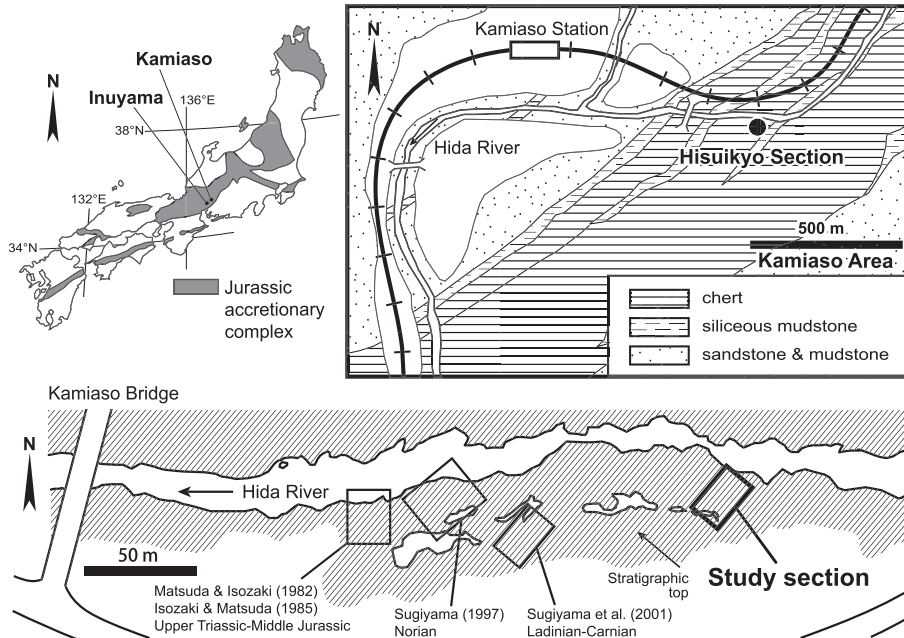


Fig. 1. Index geological sketch map (modified from Kido, 1982) of the Hisuikyo section in the Kamiaso area, central Japan (above), and the locations of the studied domains by previous and present researches on the southern bank of the Hida river (below).

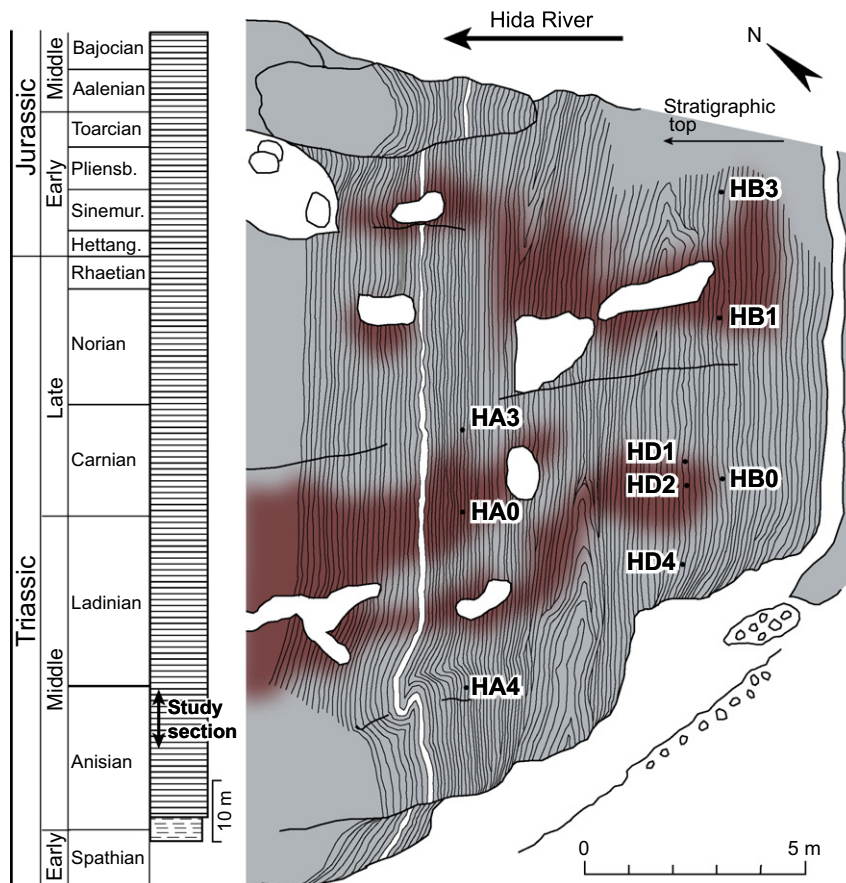


Fig. 2. Overall stratigraphic column of the Triassic–Jurassic deep-sea pelagic chert sequence at Hisuikyo (left: modified from Matsuda and Isozaki, 1991), and an enlarged sketch map of the outcrop of the studied Anisian interval with sampled beds (HB, HD, and HA) and points for geochemical analyzes (right).

anoxic cherts also have non-red dark colors. Some researchers (e.g. Ishiga et al., 1996) considered greenish-colored cherts to have deposited under intermediate conditions between oxidizing and reducing; however, this interpretation is unlikely because the transition in color occurred laterally within individual bed.

In this study, we used  $^{57}\text{Fe}$  Mössbauer spectroscopy to identify iron species and iron-bearing minerals in the Triassic bedded cherts in Japan in order to demonstrate practical differences between red and greenish gray parts within the same beds. In this article, we describe the results of identification of iron-species composition and iron-bearing minerals, and discuss effect of secondary alteration for better evaluation of primary paleo-redox signatures from deep-sea cherts.

## 2. Geologic setting and samples

The Jurassic accretionary complex is extensively exposed in the Mino-Tanba belt of Southwest Japan (e.g., Wakita, 1988; Mizutani, 1990; Isozaki, 1997b; Fig. 1). The Upper Triassic to Middle Jurassic bedded cherts are exposed in the Kamiasso area along a narrow gorge of the Hida River in the central Mino-Tanba belt (Mizutani, 1964; Igo, 1979; Kano, 1979; Kido, 1982). We collected chert samples in the Hisuikyo section in the Kamiasso area on the southern bank of the Hida River. The detailed conodont/radiolarian biostratigraphy clarified that the over 100 m-thick bedded chert of the Hisuikyo section ranges from Lower Triassic to Middle Jurassic (Kido, 1982; Matsuda and Isozaki, 1982; Isozaki and Matsuda, 1985; Matsuoaka, 1986; Sugiyama, 1997). The bedded cherts of this section are mostly red to greenish gray in color. The gradual color transition from red to greenish gray is commonly observed in the

lower half of the section at ca. 250 m to the east of the Kamiasso bridge.

We collected rock samples for geochemical analyses from the Anisian (Early Middle Triassic) interval in the lower half of the section (Fig. 2). This interval yields the Anisian conodonts (Matsuda and Isozaki, 1982) and the radiolarian assemblage of the TR2C zone of Sugiyama (1997). The bedded cherts of this interval are composed of rhythmic alternation of siliceous (ca. 5 cm thick) and argillaceous (ca. 5 mm thick) layers.

As illustrated in Fig. 3, the color of chert changes laterally from red to greenish gray within a single bed. In the transitional part between red and greenish gray, the top and bottom parts of a siliceous layer, in contact with argillaceous layer, tend to have greenish gray color, whereas the central part have red color. Photos of polished rock slabs (Fig. 4) also show the color change initiated from the contact planes with the intercalated shale. The color change is gradual between red and greenish gray parts, thus their mutual boundaries are not sharp both in outcrop and in thin section. These patterns indicate that greenish gray cherts have been derived from red cherts by secondary alteration, probably water infiltration through the intercalated shale, after the lithification.

The rock samples for analysis were collected from three nearby but different beds (Figs. 2 and 3); i.e. HA, HB and HD, within a 5-m thick interval. In order to check the change in chemical state of iron, 3 parts from each single bed were collected; i.e., red (HA0, HB1, and HD2), transitional (HA3, HB0, and HD1), and greenish gray parts (HA4, HB3, and HD4). We prepared 14 fractions from these samples for Mössbauer analysis (Fig. 4); i.e., HA0, HA3-1 (red), HA3-2, and HA4 (greenish gray) from Bed HA; HB1, HB0-1 (red), HB0-2, and HB3 (greenish gray) from

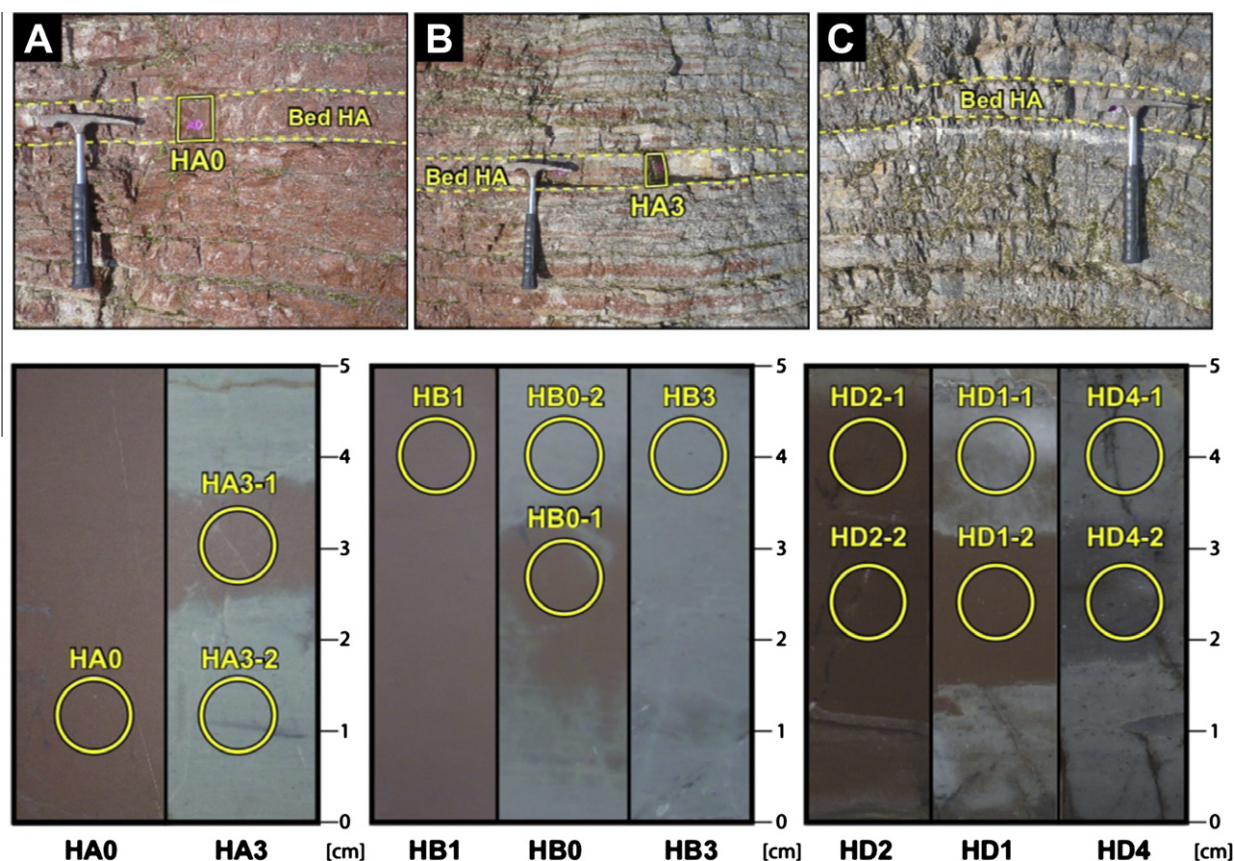


**Fig. 3.** Outcrop photographs of the samples from the chert bed HA in the Anisian interval (Fig. 2) at Hisuikyo (above); A: red part; B: red/greenish gray part; C: greenish gray part. Note the color change within the same bed occurred from red (A) to greenish gray (C), in particular, from the lower and upper bedding surfaces of chert to the interior (B). Photographs of polished rock slabs (below). For geochemical analyses including Mössbauer spectroscopy, 14 parts were collected from 3 beds; i.e., HB HD and HA (Fig. 2).

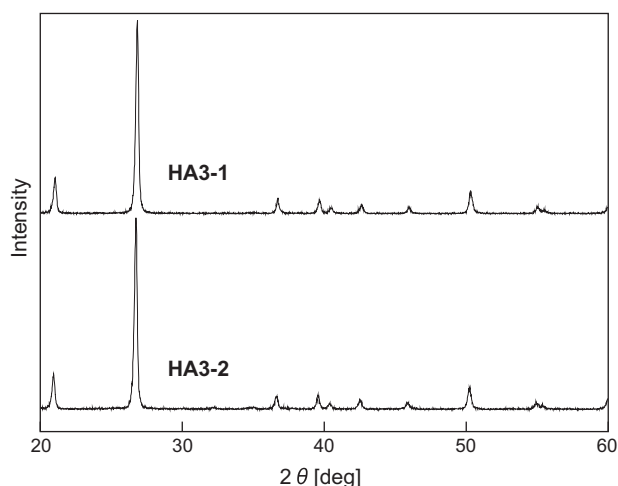


Fig. 4. XRD patterns for red chert (HA3-1) and greenish gray chert (HA3-2) from the same chert bed (HA).

Bed HB; HD2-1, HD2-2, HD1-2 (red), HD1-1, HD4-2, and HD4-1 (greenish gray) from Bed HD.

As to the color of chert, we describe in this article according to the geological rock-color chart by Munsell Color (2009); “red” in this article includes moderate reddish brown (10R 4/6), dark reddish brown (10R 3/4), moderate red (5R 4/6), dusky red (5R 3/4), moderate red (5R 5/4), grayish red (5R 4/2), and moderate brown (5YR 4/4), whereas “greenish gray” in this article corresponds to pale green (10G 6/2), greenish gray (5G 6/1), grayish blue green (5BG 5/2), pale blue (5B 6/2), light bluish gray (5B 7/1), and medium bluish gray (5B 5/1).

### 3. Analysis

In order to check the chemical state of iron in chert samples, we used X-ray diffraction (XRD) for mineralogy, X-ray fluorescent (XRF) for total amount of iron, and  $^{57}\text{Fe}$  Mössbauer spectroscopy for identification of iron species.  $^{57}\text{Fe}$  Mössbauer spectroscopy can identify chemical states of iron in powdered samples and quantify their relative abundance. The advantages of this method lie in its simplicity of analysis without chemically-destructive procedures and in higher reliability with respect to the conventional wet analysis (Matsuo et al., 2003).  $^{57}\text{Fe}$  Mössbauer spectroscopy is particularly useful in analyzing iron species in cherts composed mostly of spectroscopically transparent quartz grains, as demonstrated in Kubo et al. (1996) and Matsuo et al. (2003).

Each rock sample of chert was shaped into a slab and polished for detailed observation. For Mössbauer analysis, ca. 10 g of chert samples were crushed, and altered and/or veined parts were removed under the microscope. Then, the fresh parts were grounded to 100-mesh powder in an agate mortar. Each powdered samples of ca. 400 mg was mounted in a sample holder (16 mm in diameter, 2 mm thick). Mössbauer spectra were measured by the Austin Science S-600 Mössbauer spectrometer, in the University of Tokyo, using a 1.11 GBq  $^{57}\text{Co}/\text{Rh}$  source at room temperature (293 K). Isomer shifts (IS) were expressed with respect to the centroid of the spectrum of metallic iron foil. Mössbauer spectra were fitted by a least-squares method with restrictions of intensity and half width (HW) of peaks.

The powdered samples were also checked by XRD and XRF. For XRD analysis, we used Bruker new D8 ADVANCE at the University of Tokyo at room temperature with  $\text{Cu K}\alpha$  radiation, in  $20^\circ \leq 2\theta \leq 60^\circ$  range. For XRF analysis, we used RIGAKU SYSTEM 3550 at Tokyo Institute of Technology.

### 4. Results

Fig. 4 shows the XRD spectra of the analyzed samples. The peaks of quartz were detected ubiquitously regardless of colors of samples. Fig. 5 and Table 1 show the Mössbauer spectra, Mössbauer parameters, and total amount of iron of the 14 analyzed chert samples from the Hisuikyo section. As to the Mössbauer spectra, all samples have one sextet peak and three doublet peaks. In this study, all doublets are regarded to be symmetric. In general, the peak of pyrite ( $\text{FeS}_2$ ) and that of paramagnetic  $\text{Fe}^{3+}$  (high spin; h.s.) occur very closely from each other; however, we regard that pyrite is absent when a calculated peak area of pyrite is smaller than the detection limit, i.e. three times of the standard deviation on the baseline count. The absence of pyrite was also checked by the microscopic observation of thin sections.

According to the Mössbauer parameters, the sextet peak corresponds to hematite ( $\alpha\text{-Fe}_2\text{O}_3$ ), whereas the doublet peaks correspond to paramagnetic  $\text{Fe}^{3+}$  (h.s.) and/or two types of paramagnetic  $\text{Fe}^{2+}$  (h.s.); i.e.,  $\text{Fe}^{2+}$  (outer) with larger quadrupole splitting (QS;  $\sim 2.7$  mm/s) and  $\text{Fe}^{2+}$  (inner) with smaller QS ( $\sim 1.8$  mm/s). These results confirmed that the analyzed Middle Triassic red cherts at Hisuikyo constantly contain hematite and also  $\text{Fe}^{3+}$  (h.s.),  $\text{Fe}^{2+}$  (outer), and  $\text{Fe}^{2+}$  (inner). On the contrary, the greenish gray cherts secondarily derived from the red cherts contain  $\text{Fe}^{3+}$  (h.s.),  $\text{Fe}^{2+}$  (outer), and/or  $\text{Fe}^{2+}$  (inner) without hematite. Within individual beds, the reddish parts nearby the transition to the greenish gray parts (HA3-1, HB0-1, and HD1-2) have almost

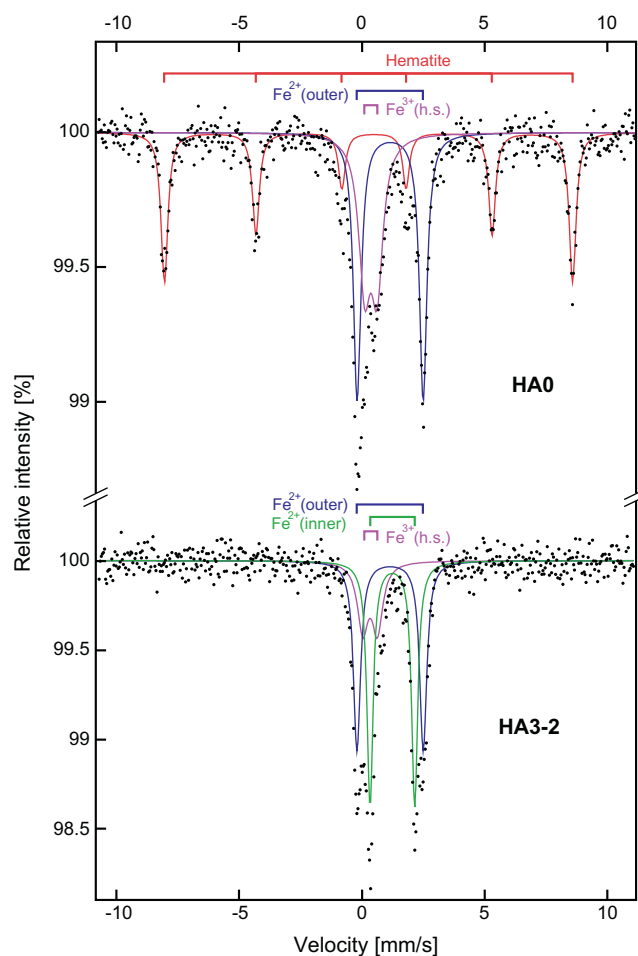


Fig. 5. Representative Mössbauer spectra of red part (HA0) and greenish gray part (HA3-2) from the same chert bed (HA).

**Table 1**  
Relative abundance of iron species and Mössbauer parameters of the Middle Triassic cherts from the Hisuikyo section in central Japan.

Sample	Color		TFe (wt.%)	Species	Area (%)	I.S. (mm/s)	Q.S. (mm/s)	H.W. (mm/s)	Hi (T)
HA0	Red	(10R 4/3)	1.6	Hematite	36.1 ± 0.5	0.37 ± 0.01	−0.22 ± 0.01	0.33 ± 0.02	51.2 ± 0.03
				Fe <sup>3+</sup> (h.s.)	28.8 ± 0.5	0.36 ± 0.01	0.51 ± 0.02	0.57 ± 0.03	
				Fe <sup>2+</sup> (outer)	35.0 ± 0.4	1.14 ± 0.00	2.67 ± 0.01	0.37 ± 0.01	
HA3-1	Red	(10R 4/6)	0.8	Hematite	25.3 ± 1.0	0.37 ± 0.01	−0.23 ± 0.02	0.33 ± 0.04	51.2 ± 0.08
				Fe <sup>3+</sup> (h.s.)	25.0 ± 1.1	0.34 ± 0.02	0.39 ± 0.05	0.63 ± 0.09	
				Fe <sup>2+</sup> (outer)	49.7 ± 1.0	1.13 ± 0.01	2.62 ± 0.01	0.40 ± 0.02	
HA3-2	Greenish gray	(5G 6/1)	1.6	Fe <sup>3+</sup> (h.s.)	20.0 ± 0.7	0.33 ± 0.03	0.60 ± 0.04	0.52 ± 0.05	
				Fe <sup>2+</sup> (outer)	37.9 ± 0.6	1.15 ± 0.01	2.70 ± 0.01	0.35 ± 0.02	
				Fe <sup>2+</sup> (inner)	42.1 ± 0.6	1.24 ± 0.00	1.82 ± 0.01	0.30 ± 0.01	
HA4	Greenish gray	(5G 6/1)	1.6	Fe <sup>3+</sup> (h.s.)	14.7 ± 0.6	0.32 ± 0.03	0.71 ± 0.05	0.56 ± 0.07	
				Fe <sup>2+</sup> (outer)	30.4 ± 0.5	1.13 ± 0.01	2.75 ± 0.01	0.40 ± 0.02	
				Fe <sup>2+</sup> (inner)	54.9 ± 0.6	1.23 ± 0.00	1.81 ± 0.01	0.30 ± 0.01	
HB1	Red	(10R 4/6)	1.0	Hematite	25.2 ± 0.5	0.38 ± 0.01	−0.24 ± 0.02	0.42 ± 0.03	51.5 ± 0.05
				Fe <sup>3+</sup> (h.s.)	21.4 ± 0.4	0.34 ± 0.01	0.66 ± 0.02	0.54 ± 0.03	
				Fe <sup>2+</sup> (outer)	37.2 ± 0.4	1.16 ± 0.00	2.72 ± 0.01	0.38 ± 0.01	
HB0-1	Red	(10R 4/6)	2.0	Hematite	25.9 ± 0.5	0.40 ± 0.01	−0.25 ± 0.02	0.44 ± 0.03	51.4 ± 0.06
				Fe <sup>3+</sup> (h.s.)	24.7 ± 0.5	0.33 ± 0.02	0.61 ± 0.02	0.51 ± 0.03	
				Fe <sup>2+</sup> (outer)	32.6 ± 0.6	1.14 ± 0.00	2.70 ± 0.01	0.36 ± 0.02	
HB0-2	Greenish gray	(5G 6/1)	1.3	Fe <sup>2+</sup> (inner)	16.9 ± 0.7	1.24 ± 0.01	1.79 ± 0.05	0.51 ± 0.06	
				Fe <sup>3+</sup> (h.s.)	19.9 ± 0.4	0.34 ± 0.01	0.64 ± 0.02	0.52 ± 0.03	
				Fe <sup>2+</sup> (outer)	37.1 ± 0.3	1.15 ± 0.00	2.71 ± 0.01	0.40 ± 0.01	
HB3	Greenish gray	(10G 6/2)	1.5	Fe <sup>2+</sup> (inner)	43.1 ± 0.3	1.24 ± 0.00	1.82 ± 0.00	0.28 ± 0.01	
				Fe <sup>3+</sup> (h.s.)	15.2 ± 0.4	0.31 ± 0.01	0.65 ± 0.02	0.50 ± 0.03	
				Fe <sup>2+</sup> (outer)	43.7 ± 0.3	1.14 ± 0.00	2.70 ± 0.01	0.38 ± 0.01	
HD2-1	Red	(5R 5/4)	1.2	Hematite	26.0 ± 0.4	0.37 ± 0.01	−0.20 ± 0.01	0.37 ± 0.02	50.9 ± 0.04
				Fe <sup>3+</sup> (h.s.)	22.0 ± 0.4	0.32 ± 0.01	0.62 ± 0.02	0.50 ± 0.03	
				Fe <sup>2+</sup> (outer)	27.5 ± 0.4	1.15 ± 0.00	2.70 ± 0.01	0.36 ± 0.01	
HD2-2	Red	(5R 5/4)	0.6	Fe <sup>2+</sup> (inner)	24.5 ± 0.4	1.23 ± 0.00	1.82 ± 0.01	0.33 ± 0.02	51.0 ± 0.11
				Hematite	18.6 ± 0.8	0.34 ± 0.02	−0.22 ± 0.03	0.37 ± 0.05	
				Fe <sup>3+</sup> (h.s.)	17.2 ± 0.9	0.31 ± 0.06	0.61 ± 0.08	0.66 ± 0.11	
HD1-2	Red	(5R 5/4)	–	Fe <sup>2+</sup> (outer)	49.7 ± 1.0	1.14 ± 0.00	2.64 ± 0.01	0.34 ± 0.02	51.1 ± 0.10
				Fe <sup>2+</sup> (inner)	14.5 ± 1.0	1.23 ± 0.02	1.78 ± 0.06	0.42 ± 0.09	
				Hematite	37.3 ± 1.3	0.36 ± 0.02	−0.18 ± 0.03	0.44 ± 0.05	
HD1-1	Greenish gray	(10G 6/2)	1.3	Fe <sup>3+</sup> (h.s.)	15.3 ± 1.1	0.29 ± 0.06	0.71 ± 0.09	0.53 ± 0.11	
				Fe <sup>2+</sup> (outer)	28.1 ± 1.2	1.17 ± 0.01	2.71 ± 0.02	0.32 ± 0.03	
				Fe <sup>2+</sup> (inner)	19.4 ± 1.4	1.25 ± 0.02	1.90 ± 0.11	0.52 ± 0.12	
HD4-1	Greenish gray	(5G 7/1)	1.3	Fe <sup>3+</sup> (h.s.)	18.5 ± 0.4	0.33 ± 0.01	0.66 ± 0.02	0.52 ± 0.03	
				Fe <sup>2+</sup> (outer)	57.0 ± 0.4	1.14 ± 0.00	2.67 ± 0.01	0.37 ± 0.01	
				Fe <sup>2+</sup> (inner)	24.5 ± 0.4	1.23 ± 0.00	1.82 ± 0.01	0.35 ± 0.02	
HD4-2	Greenish gray	(5G 5/1)	0.4	Fe <sup>3+</sup> (h.s.)	15.9 ± 0.3	0.35 ± 0.01	0.63 ± 0.02	0.51 ± 0.03	
				Fe <sup>2+</sup> (outer)	49.2 ± 0.3	1.14 ± 0.00	2.67 ± 0.00	0.37 ± 0.01	
				Fe <sup>2+</sup> (inner)	34.9 ± 0.3	1.24 ± 0.00	1.81 ± 0.00	0.30 ± 0.01	
				Fe <sup>3+</sup> (h.s.)	13.9 ± 0.7	0.33 ± 0.03	0.65 ± 0.06	0.45 ± 0.07	
				Fe <sup>2+</sup> (outer)	62.6 ± 0.8	1.14 ± 0.00	2.66 ± 0.01	0.35 ± 0.01	
				Fe <sup>2+</sup> (inner)	23.5 ± 0.7	1.24 ± 0.01	1.83 ± 0.03	0.34 ± 0.04	

the same iron composition as the red parts (HA0, HB1, and HD2-2, respectively). Likewise the greenish gray parts nearby the color transition (HA3-2, HB0-2, and HD1-1) have almost the same iron composition as the greenish gray parts (HA4, HB3, and HD4-1, respectively). These results confirmed that the color of chert precisely reflects the chemical state of iron in it.

## 5. Discussion

### 5.1. Change in color from red to greenish gray

#### 5.1.1. Iron species

The XRF data shown in Table 1 clearly demonstrate that the total amount of iron in deep-sea chert is relatively small with respect to total silica, less than 2 wt.%, regardless of colors. The present XRD analysis could not identify iron-bearing minerals in the samples because of the scarcity of iron; however, it is noteworthy that the red and greenish gray parts from the same bed have no significant difference in total iron contents. These results indicate that the color change from red to greenish gray was related not to iron loss, such as by preferential leaching of iron, but to the decompo-

sition and recrystallization of iron-bearing mineral clearly after the deposition/consolidation.

The Mössbauer spectroscopic data clearly demonstrate the difference in iron species between the red and greenish gray parts from the same chert beds. The red cherts are characterized solely by hematite, whereas Fe<sup>3+</sup>(h.s.) and Fe<sup>2+</sup>(outer) occur abundantly from the greenish gray chert. The iron species of the analyzed red and greenish gray cherts are shown in Fig. 6. It is difficult to specifically identify minerals that contain Fe<sup>3+</sup>(h.s.), Fe<sup>2+</sup>(outer) or Fe<sup>2+</sup>(inner) by Mössbauer analysis; however, they can be distinguished from each other based on the Mössbauer parameters. Fe<sup>3+</sup>(h.s.) and Fe<sup>2+</sup>(outer) are likely included in clay minerals such as illite or chlorite. Fe<sup>2+</sup>(inner) may correspond to amorphous siderite (FeCO<sub>3</sub>)-like mineral.

From all analyzed chert samples, pyrite was not detected at all. Absence of pyrite was also confirmed by microscopic observation of the thin sections. The results of Mössbauer analysis indicate that the color change from red to greenish gray corresponds not only to the loss of hematite but also to the relative increase of Fe<sup>2+</sup>(inner) and/or Fe<sup>2+</sup>(outer). The relative abundance of Fe<sup>3+</sup>(h.s.) does not show large fluctuation through the alteration.

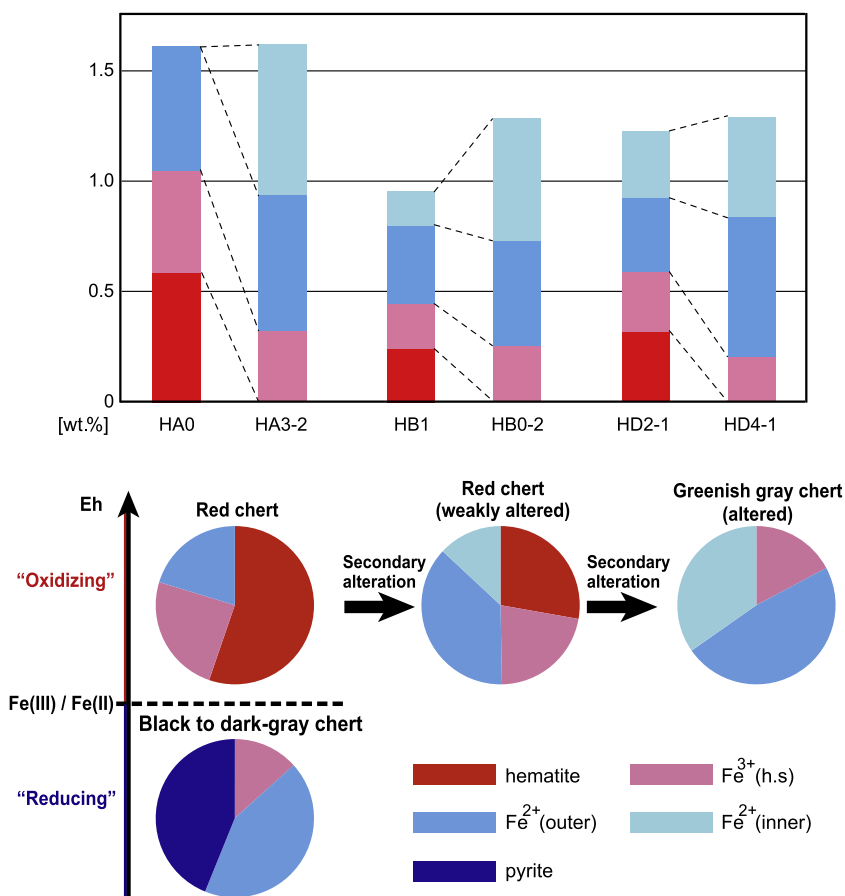


**Fig. 6.** Relative abundance among individual iron species of red and greenish gray cherts at Hisuikyo (above) and comparison of averaged abundance among iron species of red, greenish gray and black to dark-gray cherts (below). A pair of red part and greenish gray part from the same chert bed was analyzed for 3 distinct chert beds; HA (HA0 and HA3-2), HB (HB1 and HB3), and HD (HD2-2 and HD4-2), respectively. Red chert primarily deposited in an oxidizing condition constantly contains hematite as the main iron species, whereas black to dark-gray chert deposited in a reducing condition contains pyrite. The amount of hematite decreases, instead that of Fe<sup>2+</sup> (inner) increases through the secondary alteration from red to greenish gray chert. The data of red chert and black to dark-gray chert are compiled from Kubo et al. (1996) and Matsuo et al. (2003).

Concerning the colors of chert, the red color is likely derived from abundant hematite within nearly transparent quartz, as already pointed out by the previous works (Nakao and Isozaki, 1994; Kubo et al., 1996; Matsuo et al., 2003). On the other hand, we cannot specifically identify the responsible mineral for the greenish colors. Kubo et al. (1996) and Matsuo et al. (2003) speculated that illite and/or chlorite common in chert might be possible carriers of Fe<sup>2+</sup>(outer), and the latter naturally provide greenish colors. Meanwhile, siderite is variable in color and often shows greenish colors, therefore, the siderite-like mineral with Fe<sup>2+</sup>(inner) may similarly gives greenish colors. If this is the case, the color change from red to greenish gray may reflect the decomposition of hematite paired with the new formation of the Fe<sup>2+</sup>(inner)-bearing siderite-like mineral, although further research is needed for identifying the origin of the greenish colors.

### 5.1.2. Redox evaluation

In a series of the <sup>57</sup>Fe Mössbauer studies (Kubo et al., 1996; Matsuo et al., 2003; Sato et al., 2009), we set the redox potential of the Fe(III)/Fe(II) transition (Berner, 1981) for the threshold in distinguishing the “red state” and “black to dark-gray state” of chert. Here, we use “oxidizing” or “reducing” for describing redox potentials higher or lower than that of the Fe(III)/Fe(II) transition, respectively. The redox potential of this threshold was given at 70–80 eV in a model seawater by Thomson et al. (1993). The chemical states of iron in deep-sea cherts suggest the redox of interstitial water in deep-sea sediments at the time when the chemical

system was closed before the lithification. Although the quantitative assignment of paleo-redox appears difficult, the presence of hematite or pyrite in pelagic deep-sea cherts can tell us approximately whether the primary depositional environment was oxidizing or reducing.

Previous studies of deep-sea chert demonstrated the clear difference in relative redox between red hematite-bearing cherts and black to dark-gray pyrite-bearing ones (e.g. Nakao and Isozaki, 1994; Kubo et al., 1996; Matsuo et al., 2003). Table 2 lists the average iron-species compositions of the red and black to dark-gray cherts for comparison. After Kubo et al. (1996) and Matsuo et al. (2003), the values for typical red chert represent those of the Lower Permian and Upper Triassic “brick red cherts”, whereas those for typical black to dark-gray chert represent the Upper Permian and Lower Triassic “gray” and “black” cherts.

Table 2 also lists the present data of average iron composition of red part, greenish gray part from Hisuikyo. It is clear that the typical red cherts never contain Fe<sup>2+</sup>(inner). In contrast, the reddish cherts from Hisuikyo have lesser amount of hematite than the typical red chert, and they contain Fe<sup>2+</sup>(inner). These facts suggest that the secondary iron alteration may have slightly affected also the red cherts from Hisuikyo. We confirmed that the greenish gray cherts from Hisuikyo were obviously derived from primary red hematite-bearing cherts. We interpret that this variation in chemical states of iron demonstrates the gradational aspects of the secondary alteration from a non-altered red chert to a considerably altered greenish gray chert, via a transitional reddish chert (Fig. 6).

**Table 2**

Average abundance (%) among individual iron species of red, greenish gray, and black to dark-gray cherts. Data for red and black to dark-gray cherts are compiled from Kubo et al. (1996) and Matsuo et al. (2003), whereas those for altered chert are the averaged values of red and greenish gray cherts clarified in the present study at Hisuikyo in central Japan.

Color	Fe <sup>3+</sup>		Fe <sup>2+</sup>		
	Hematite	Fe <sup>3+</sup> (h.s.)	Fe <sup>2+</sup> (outer)	Fe <sup>2+</sup> (inner)	Pyrite
Red	55.2	24.5	20.4	–	–
Black to dark-gray	–	13.4	42.8	–	43.8
Red (weakly altered)	27.8	22.0	37.1	13.1	–
Greenish gray (altered)	–	17.2	47.9	34.8	–

In general, deep-sea cherts do not contain carbonate minerals due to their depositional setting deeper than the carbonate compensation depth (Matsuda and Isozaki, 1991). Although the occurrence of some carbonate, such as amorphous siderite-like minerals, is suggested by Fe<sup>2+</sup>(inner) in the altered cherts, they were likely formed in the secondary alteration. In this regard, the detection of Fe<sup>2+</sup>(inner) and their relative abundance may be used an index of secondary alteration.

Well-preserved red chert with more than 50% of hematite does not contain Fe<sup>2+</sup>(inner) at all, whereas weakly altered red chert with less than 30% of hematite contains ~20% of Fe<sup>2+</sup>(inner) and altered greenish gray chert contains nearly 40% of Fe<sup>2+</sup>(inner) without hematite. This correlation between hematite and Fe<sup>2+</sup>(inner) suggests that iron from decomposed hematite was attached to the siderite-like mineral as Fe<sup>2+</sup>(inner) during the secondary alteration.

In short, the present result demonstrated a typical pattern of secondary alteration of ancient deep-sea chert in accretionary complex; namely the primary red chert deposited under oxidizing conditions in open ocean are secondarily changed into greenish gray ones by decomposing hematite and transforming the freed irons into Fe<sup>2+</sup>(inner) under more reducing conditions in rocks.

## 5.2. Greenish gray chert vs. black chert

As all analyzed samples indicate, red cherts never yield pyrite nor even altered greenish gray cherts, neither, except for the faulted and/or veined portions. Thus, most of the Late Paleozoic to Mesozoic deep-sea cherts, showing red or greenish gray color, are presumed to contain no pyrite. The deposition of pyrite-bearing cherts is very rare and abnormal in the geological history. Only the black to dark-gray cherts around the P–T boundary and the Toarcian event horizons have pyrites (Nakao and Isozaki, 1994; Hori, 1993). These were regarded to indicate the past development of reducing conditions in open oceans, which was unique to some extinction-related boundaries. The black to dark-gray cherts across the P–T boundary and the Toarcian event have framboidal pyrites that suggests reducing conditions developed in the overlying water column (Algeo et al., 2011).

In terms of chemical states of iron, here we compare the primary black to dark-gray cherts from the P–T boundary interval and the secondary altered non-reddish cherts examined in this study (Fig. 6). Through the comparison, the difference between them becomes clear; the altered greenish gray cherts are dominated by Fe<sup>2+</sup>(inner) without pyrite, whereas the P–T boundary black cherts solely by pyrite without Fe<sup>2+</sup>(inner). As there is no intermediate example with co-occurrence of pyrite and Fe<sup>2+</sup>(inner) in the hitherto analyzed samples, this difference in chemical state of iron can be a criterion to discriminate these two types of non-reddish cherts, although these look alike each other in the outcrop. As long as the greenish gray cherts are of secondary alteration origin, they do not record the primary redox information for the past oceans.

Matsuo et al. (2003) reported the apparent co-occurrence of siderite (iron-bearing carbonate) with pyrite in the gray siliceous/car-

bonaceous claystones near the P–T boundary that appears contradictory with the above conclusion from this study. In terms of Mössbauer parameters, however, the siderite reported by Matsuo et al. (2003) (IS = 1.24 mm s<sup>-1</sup>, QS = 1.50 mm s<sup>-1</sup>) is clearly distinguished from the siderite-like material observed in this study (IS = ~1.24 mm s<sup>-1</sup>, QS = ~1.82 mm s<sup>-1</sup>). The P–T boundary claystones are known to have primary pyrite but no primary hematite nor siderite (carbonate) because of the deposition under anoxic conditions below the carbonate compensation depth (Isozaki, 1997a). The siderite in them is regarded as a secondary diagenetic product never essentially co-occurred with pyrite. After all, the siderite in the P–T boundary claystones is clearly different not only in Mössbauer parameters but also in origin from the siderite-like mineral derived from hematite in the studied samples.

We can conclude that the investigation of chemical state of iron in cherts by Mössbauer analysis is effective in checking not only primary paleo-redox but also the degree of secondary alteration. In reconstructing paleo-redox from ancient chert, checking chemical state of iron and composition of iron species appears necessary, besides other proxies, such as REE abundance pattern, pyrite morphology, etc.

## 6. Summary

We conducted <sup>57</sup>Fe Mössbauer spectroscopic investigation of Middle Triassic pelagic deep-sea cherts at Hisuikyo in central Japan, in order to check the geochemical signature for the color change within a single bed from the primary red to secondary altered greenish gray. By the analysis on chemical state of iron in chert for 14 samples, the following results were obtained (Fig. 7).

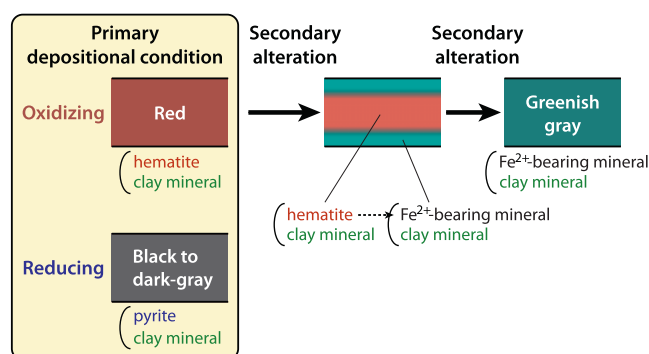


**Fig. 7.** Schematic diagram showing the possible process of secondary alteration of deep-sea chert. Red chert primarily deposited in an oxidizing primary setting commonly with hematite. During secondary alteration, however, hematite is usually decomposed and the excess iron is incorporated into another Fe<sup>2+</sup>-bearing mineral, such as siderite. Along this process, the primary red color is lost and, in turn, a greenish gray color appears likely reflecting the emergence of chlorite in the background. In contrast, primary black to dark-gray pyrite-bearing chert deposited in an anoxic condition is not involved in such color change from red to greenish gray.

- (1) The red chert samples constantly contain hematite,  $\text{Fe}^{3+}$ (h.s.),  $\text{Fe}^{2+}$ (outer) and  $\text{Fe}^{2+}$ (inner), whereas the greenish gray ones contain  $\text{Fe}^{3+}$ (h.s.),  $\text{Fe}^{2+}$ (outer) and  $\text{Fe}^{2+}$ (inner).
- (2) The greenish gray cherts contain a larger amount of  $\text{Fe}^{2+}$ (inner) than the red cherts from the same single bed, without hematite. This suggests that hematite has been decomposed and the freed iron has changed into  $\text{Fe}^{2+}$ (inner) during the secondary alteration probably along with the color change from red to greenish gray.
- (3) The secondary altered greenish gray cherts can be clearly distinguished from the black to dark-gray chert from the Permian–Triassic boundary and the Toarcian event horizons, which were deposited primary in reducing condition.

## Acknowledgements

Yasuhiro Kato and an anonymous reviewer provided constructive comments on the original manuscript. Tsuyoshi Komiya helped us with XRF analysis. Masayuki Ikeda helped us in fieldwork. The members of Komaba Earth Science Group in the University of Tokyo provided valuable discussions. This research was supported by a Grant-in-Aid of the Japan Society of Promoting Science (Nos. 16204040, 20224012) and the Global-COE program “From the Earth to Earths”.

## References

- Algeo, T.J., Kuwahara, K., Sano, H., Bates, S., Lyons, T., Elswick, E., Hinnov, L., Ellwood, B., Moser, J., Maynard, J.B., 2011. Spatial variation in sediment fluxes, redox conditions, and productivity in the Permian–Triassic Panthalassic Ocean. *Palaeogeography, Palaeoclimatology, Palaeoecology* 308, 65–83.
- Anbar, A.D., Knoll, A.H., 2002. Proterozoic ocean chemistry and evolution: a bioinorganic bridge? *Science* 297, 1137–1142.
- Berner, R.A., 1981. A new geochemical classification of sedimentary environments. *Journal of Sedimentary Petrology* 51, 359–365.
- Holland, H.D., 2006. The oxygenation of the atmosphere and oceans. *Philosophical Transactions of the Royal Society B* 361, 903–915.
- Hori, R., 1993. Toarcian oceanic event in deep-sea sediments. *Bulletin of the Geological Survey of Japan* 44, 555–570 (in Japanese with English abstract).
- Igo, H., 1979. Conodont biostratigraphy and restudy of geological structure at the eastern part of Mino Belt. In: *Biostratigraphy of Permian and Triassic Conodonts and Holothurian Sclerites in Japan*, pp. 103–113. (Prof. M. Kanuma memorial volume of retirement) (in Japanese).
- Ishiga, H., Ishida, K., Dozen, K., Musashino, M., 1996. Geochemical characteristics of pelagic chert sequences across the Permian–Triassic boundary in southwest Japan. *The Island Arc* 5, 180–193.
- Isozaki, Y., 1994. Superanoxia across the Permo-Triassic boundary: record in accreted deep-sea pelagic chert in Japan. *Canadian Society of Petroleum Geologists Memoir* 17, 805–812.
- Isozaki, Y., 1997a. Permo-Triassic boundary superanoxia and stratified super ocean: records from lost deep sea. *Science* 276, 235–238.
- Isozaki, Y., 1997b. Jurassic accretion tectonics in Japan. *The Island Arc* 6, 25–51.
- Isozaki, Y., Matsuda, T., 1985. Early Jurassic radiolarians from bedded chert in Kamiaso, Mino belt, Central Japan. *Earth Science* 39, 429–442.
- Kajiwara, Y., Yamakita, S., Ishida, K., Ishiga, H., Imai, A., 1994. Development of a largely anoxic stratified ocean and its temporary massive mixing at the Permian/Triassic boundary supported by the sulfur isotopic record. *Palaeogeography, Palaeoclimatology, Palaeoecology* 111, 367–379.
- Kakuwa, Y., 2008. Evaluation of palaeo-oxygenation of the ocean bottom across the Permian–Triassic boundary. *Global and Planetary Change* 63, 40–56.
- Kano, K., 1979. Giant deckenpaket and olistostrome in the eastern Mino district, central Japan. *Journal of the Faculty of Science, Univ Tokyo, Section II* 20, 31–59.
- Kato, Y., Nakao, K., Isozaki, Y., 2002. Geochemistry of late Permian to early Triassic pelagic cherts from southwest Japan: implications for an oceanic redox change. *Chemical Geology* 182, 15–34.
- Kido, S., 1982. Occurrence of Triassic chert and Jurassic siliceous shale at Kamiaso, Gifu prefecture, central Japan. *News of Osaka Micropaleontology Special* 5, 135–151 (in Japanese with English abstract).
- Kubo, K., Isozaki, Y., Matsuo, M., 1996. Color of bedded chert and redox condition of depositional environment:  $^{57}\text{Fe}$  Mössbauer spectroscopic study on chemical state of iron in Triassic deep-sea pelagic chert. *Journal of Geological Society of Japan* 102, 40–48 (in Japanese with English abstract).
- Matsuda, T., Isozaki, Y., 1982. Radiolarians around the Triassic–Jurassic boundary from the bedded chert in the Kamiaso Area, Southwest Japan. Appendix: “Anisian” radiolarians. *News of Osaka Micropaleontology Special* 5, 93–101 (in Japanese with English abstract).
- Matsuda, T., Isozaki, Y., 1991. Well-documented travel history of Mesozoic pelagic chert in Japan: from remote ocean to subduction zone. *Tectonics* 10, 475–499.
- Matsuo, M., Kubo, K., Isozaki, Y., 2003. Mössbauer spectroscopic study on characterization of iron in the Permian to Triassic deep-sea chert from Japan. *Hyperfine Interaction (C)* 5, 435–438.
- Matsuoka, A., 1986. Stratigraphic distribution of two species of *Tricolocapsa* in the Hisuikyo section of the Kamiaso area, Mino Terrane. *News of Osaka Micropaleontologists, Special* 7, 59–62 (in Japanese with English abstract).
- Mizutani, S., 1964. Superficial folding of the Paleozoic system of central Japan. *Journal of Earth Science, Nagoya University* 12, 17–83 (pls1–5).
- Mizutani, S., 1990. Mino terrane. In: Ichikawa, K., Mizutani, S., Hara, I., Hada, S., Yao, A. (Eds.), *Pre-Cretaceous Terranes of Japan*. Special Publication of IGCP #224, Osaka, pp. 121–135.
- Munsell color, 2009. Geological rock-color chart.
- Nakao, K., Isozaki, Y., 1994. Recovery history from the P/T boundary deep-sea anoxia recorded in pelagic chert in the Inuyama area, Mino Belt, Southwest Japan. *Journal of Geological Society of Japan* 100, 505–508 (in Japanese).
- Sato, T., Isozaki, Y., Matsuo, M., 2009. Redox conditions of the deep ocean in the late Neoproterozoic–early Paleozoic:  $^{57}\text{Fe}$  Mössbauer spectroscopic study on deep-sea pelagic chert. *Journal of Geological Society of Japan* 115, 391–399 (in Japanese with English abstract).
- Shields, G., Och, L., 2011. The case for a neoproterozoic oxygenation event: geochemical evidence and biological consequences. *GSA Today* 21, 4–11.
- Sugiyama, K., 1997. Triassic and lower Jurassic radiolarian biostratigraphy in the siliceous claystone and bedded chert units of the southeastern Mino terrane, central Japan. *Bulletin of Mizunami Fossil Museum* 24, 79–193.
- Thomson, J., Higgs, N.C., Croudace, I.W., Colley, S., Hydes, D.J., 1993. Redox zonation of elements at an oxic/post-oxic boundary in deep-sea sediments. *Geochimica Cosmochimica Acta* 57, 579–595.
- Thurston, D.R., 1972. Studies on bedded cherts. *Contributions to Mineralogy and Petrology* 36, 329–334.
- Umeda, M., 1999. The crystallinity index for the quartz of the Triassic red-blue striped chert in Nanjo Massif, Fukui Prefecture, central Japan. *Bulletin of the Fukui City Museum of Natural History* 46, 77–87 (in Japanese with English abstract).
- Wakita, K., 1988. Origin of chaotically mixed rock bodies in the early Jurassic to early cretaceous sedimentary complex of the Mino Terrane, central Japan. *Bulletin of the Geological Survey of Japan* 39, 675–757.